

Organotin Biocides. Part 11.¹ Triphenyltin Benzoates: Electronic *versus* Steric Control of Structure

Kieran C. Molloy*

School of Chemistry, University of Bath, Claverton Down, Bath BA2 7AY

Stephen J. Blunden and Robin Hill

International Tin Research Institute, Kingston Lane, Uxbridge, Middlesex UB8 3PJ

Twenty four triphenyltin derivatives of substituted benzoic acids have been synthesised. On the basis of i.r., ¹¹⁹Sn n.m.r., and Mössbauer spectroscopic data, structures have been assigned to these compounds as either tetrahedral monomers or *trans*-SnR₃O₂ polymers. The choice of structure in these systems is dictated by both steric and electronic effects, and for two compounds (2,6-dichloro- and 2-nitro-benzoates) evidence suggests that both structures occur. The factors which influence the preferred structure are discussed.

Despite being intensively studied over the last decade, the factors influencing the choice of solid-state structure for organotin carboxylates between four- or five-co-ordinated monomers [(I),(II)] or a five-co-ordinated polymer (III) are still not fully understood.

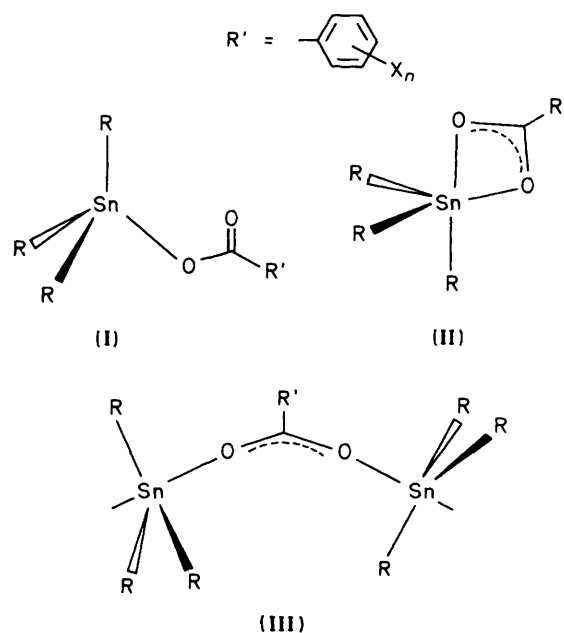
In some of the earliest reports^{2,3} on these systems, the steric influence of the hydrocarbon groups on either tin or the carboxylic acid was noted, *i.e.* steric bulk at R or R' (by, for example, chain branching) results in the monomer (I), rather than the polymer (III). More recently, we have compared the structures of triphenyltin formate and acetate, and have highlighted those structural features within the polymer chain which are most susceptible to steric influence and which ultimately give rise to (I), at least as far as aliphatic carboxylic acid derivatives are concerned.⁴ Collective crystallographic data endorse a clear preference for (III), but surprisingly, few examples of tetrahedral,⁵ distorted tetrahedral,^{6,7} or chelated⁸ structures have been reported.

Our interest in the structure/activity relationships for biocidally active organotin compounds (ref. 1 and refs. therein) has caused us to focus our attention on this structural problem, since in certain cases compounds of structure (II) show diminished activity with respect to similar species adopting structures (I) or (III).⁹ In a spectroscopic study of triphenyltin benzoates, we noted that for various substituents on the benzoate ring (2-OH, 4-OH, 2-OMe, 3-Cl, 4-Cl *etc.*) structure (I) was preferred, but in the case of 2-chlorobenzoic acid, the triphenyltin ester has polymeric structure (III).¹⁰ These initial results suggested to us that electronic factors also play a role in structure determination, and that an interplay between the three structures could be achieved by variation in X. The recent report by Holmes *et al.*¹¹ on the structures of the monomeric 4-chlorobenzoate (I; X_n = 4-Cl) and polymeric 2-chlorobenzoate (III; X_n = 2-Cl) confirms our structural proposals,¹⁰ and these authors also note the possibility that electronic factors are dictating structures. In the light of this report we now present spectroscopic data for a wide range of triphenyltin benzoates and assess in detail the competition between steric and electronic influences upon structure.

Experimental

Tin-119 n.m.r. spectra were recorded under nuclear Overhauser suppressed conditions, in 10-mm tubes on a JEOL FX60Q spectrometer, with field frequency lock to external D₂O. Tin-119 chemical shifts are relative to SnMe₄ and are accurate to ±0.1 p.p.m.

Infrared spectra were recorded in the 4 000—200 cm⁻¹ region



on Perkin-Elmer 1330 or 599B instruments as Nujol mulls, KBr discs, or CCl₄ solutions (0.2 g in 3.0 cm³).

Tin-119 Mössbauer spectra, at 78 K and also in variable-temperature experiments, were obtained under previously reported conditions.^{10,12} Isomer shift data are relative to SnO₂. In the variable-temperature Mössbauer experiments, samples containing 0.8—1.0 mg ¹¹⁹Sn cm⁻² were used to minimise thickness effects, while allowing statistically acceptable spectra to be accumulated in 12—24 h.

Compounds were synthesised by reacting SnPh₃OH with an equimolar quantity of the appropriate carboxylic acid in either acetone (route 1) or toluene, using a Dean and Stark separator (route 2), as described previously.¹⁰ Details of the preparative method and recrystallisation solvents are given in Table 1.

Discussion

Twenty four triphenyltin esters of substituted benzoic acids have been synthesised, and their structures probed in solution and in the solid state by i.r., ¹¹⁹Sn n.m.r., and ¹¹⁹Sn Mössbauer spectroscopy (Table 2). The structures of these compounds fall into three groups. Compounds (1)—(17) all have quadrupole splitting (q.s.) values in the range 2.30—2.76 mm s⁻¹, which can

Table 1. Analytical data^a for triphenyltin benzoates, SnPh₃(O₂CC₆H_{5-n}X_n)

Compound	X _n	Preparation	C	H	N	Sn	M.p. (°C)	m/e ^b
(1)	2-H ^c	1	63.6 (63.7)	4.4 (4.3)		25.1 (25.3)	85—87	
(2)	4-SMe ^c	2	60.6 (60.4)	4.4 (4.3)		23.4 (23.0)	143—145	
(3)	2-NH ₂ ^c	2	61.4 (61.7)	4.5 (4.3)	2.9 (3.9)	23.9 (24.5)	110—112	
(4)	4-OH ^c	1	62.3 (61.6)	4.2 (4.1)		24.5 (24.4)	141—143	
(5)	2-Me ^c	1	63.9 (64.3)	4.5 (4.5)		24.4 (24.5)	68—70	
(6)	2-OMe ^c	2	62.3 (62.3)	4.5 (4.4)		23.6 (23.7)	110—112	
(7)	2-F ^d	2	61.3 (61.4)	3.8 (3.9)		22.8 (24.3)	65	490 ^e
(8)	3-F ^d	1	61.4 (61.4)	3.9 (3.9)		24.3 (24.3)	94—96	490 ^e
(9)	4-F ^d	1	61.4 (61.4)	3.9 (3.9)		24.0 (24.3)	93—95	413 ^f
(10)	3-Cl ^e	1	59.4 (59.4)	3.9 (3.8)		23.7 (23.5)	88—90	
(11)	4-Cl ^e	1	59.0 (59.4)	3.7 (3.8)		23.5 (23.5)	128—135	
(12)	2,5-Cl ₂ ^g	2	54.5 (55.6)	3.5 (3.4)		21.8 (22.0)	121—123	505 ^h
(13)	3,4-Cl ₂ ⁱ	2	55.5 (55.6)	3.3 (3.4)		22.5 (22.0)	98—99	463 ^f
(14)	3,5-Cl ₂ ⁱ	2	55.4 (55.6)	3.4 (3.4)		22.0 (22.0)	139—140	540 ^e
(15)	3-NO ₂ ^d	1	58.2 (58.2)	3.8 (3.7)	2.7 (2.7)	23.1 (23.0)	92—94	j
(16)	4-NO ₂ ^d	1	58.4 (58.2)	3.8 (3.7)	2.7 (2.7)	22.7 (23.0)	151—153	517 ^e
(17)	3,5-(NO ₂) ₂	1	53.5 (53.5)	3.4 (3.2)	4.9 (5.0)	20.8 (21.2)	168—170	562 ^e
(18)	2-Cl ^e	2	58.7 (59.4)	3.8 (3.8)		23.5 (23.5)	58—60 ^k	
(19)	2-Br ^g	2	54.0 (54.6)	3.6 (3.5)		21.3 (21.6)	48	475 ^f
(20)	2-I ^g	1	49.8 (50.3)	3.3 (3.2)		20.5 (20.3)	68—70	521 ^f
(21)	2,4-Cl ₂ ^{g,i}	2	55.0 (55.6)	3.4 (3.4)		21.4 (22.0)	100—103	505 ^h
(22)	2,3-Cl ₂ -0.5Me ₂ CO ^{g,m}	1	56.2 (56.0)	3.7 (3.7)		20.6 (20.9)	105—106	505 ^h
(23)	2,6-Cl ₂ -0.5C ₆ H ₁₂ ^{m,n}	2	57.5 (57.8)	4.2 (4.2)			92—94	540 ^e
(24a)	2-NO ₂ ^d	1,2	57.9 (58.2)	3.7 (3.7)	2.6 (2.7)	22.8 (23.1)	105—106	
(24b)	2-NO ₂ -0.25C ₆ H ₁₂ ^{g,m}	1,2	58.9 (59.2)	3.8 (4.1)	2.7 (2.6)		85	487 ^o

^a Calculated values in parentheses. ^b Highest observed mass fragment. ^c Prepared previously (ref. 10). ^d Recrystallised from toluene–light petroleum. ^e Parent ion (*M*). ^f *M* – C₆H₅. ^g Recrystallised from acetone–light petroleum (b.p. 40–60°C). ^h *M* – Cl. ⁱ Recrystallised from cyclohexane. ^j Very weak mass spectrum. Mass of highest assignable fragment 154 (C₆H₅–C₆H₅). ^k Reported as 79–82°C (ref. 11). ^l ¹H N.m.r. indicates inclusion of traces of Me₂CO in solid. ^m From ¹H n.m.r. integrals. ⁿ Recrystallised from acetone–cyclohexane. ^o *M* – NO – 0.25C₆H₁₂.

Table 2. Infrared, ¹¹⁹Sn n.m.r., and ¹¹⁹Sn Mössbauer data for SnPh₃(O₂CC₆H_{5-n}X_n)

Compound	X _n	v _{asym} (CO ₂) (solid, ^a solution ^b)	δ(¹¹⁹ Sn)	I.s. ^c	Q.s. ^c	pK _a ^d
(1)	2-H	1 622, 1 618	–114.3	1.24	2.55	4.20
(2)	4-SMe	1 628, 1 636	–115.6	1.27	2.42	4.20
(3)	2-NH ₂	1 615, 1 622	–119.5	1.21	2.44	4.91
(4)	4-OH	1 605, 1 605	–114.5	1.31	2.55	4.58
(5)	2-Me	1 625, 1 628	–119.9	1.25	2.42	3.91
(6)	2-OMe	1 629, 1 628	–121.9	1.25	2.30	4.08
(7)	2-F	1 635, 1 630	–108.9	1.28	2.35	3.27
(8)	3-F	1 623, 1 634	–107.1	1.23	2.39	3.86
(9)	4-F	1 620, (1 635, 1 625)	–110.7	1.23	2.37	4.14
(10)	3-Cl	1 627, 1 638	–105.9	1.27	2.42	3.83
(11)	4-Cl	1 628, 1 638	–108.2	1.24	2.36	3.92
(12)	2,5-Cl ₂	1 641, 1 639	–99.5	1.26	2.47	2.55
(13)	3,4-Cl ₂	1 639, 1 635	–103.0	1.21	2.37	3.59
(14)	3,5-Cl ₂	1 648, 1 635	–100.2	1.25	2.51	3.46
(15)	3-NO ₂	1 629, 1 640	–97.9	1.26	2.54	3.46
(16)	4-NO ₂	1 633, 1 643	–97.7	1.26	2.54	3.42
(17)	3,5-(NO ₂) ₂	(1 648, 1 620), 1 655	–84.9	1.29	2.76	2.72
(18)	2-Cl	1 540, 1 640	–106.3	1.34	3.71	2.92
(19)	2-Br	1 540, 1 637	–105.9	1.31	3.70	2.85
(20)	2-I	1 543, 1 635	–105.1	1.33	3.49	2.86
(21)	2,4-Cl ₂	1 540, 1 635	–102.1	1.33	3.56	2.68
(22)	2,3-Cl ₂ -0.5Me ₂ CO	1 550, 1 650	–100.6	1.33	3.56	2.55
(23)	2,6-Cl ₂ -0.5C ₆ H ₁₂	1 653, ^e 1 660	–93.0	1.32	2.57	1.64
(24a)	2-NO ₂	1 645, 1 650	–92.8	1.29	2.58	2.21
(24b)	2-NO ₂ -0.25C ₆ H ₁₂	1 520, 1 653	–91.6	1.33	3.70	2.21

^a KBr disc unless indicated otherwise. ^b CCl₄ solutions. ^c Values in mm s⁻¹ (±0.04 mm s⁻¹). ^d Ref. 16. ^e 1 545 cm⁻¹ as Nujol mull.

arise from either structural type (I) or (II).¹³ For this group of compounds, v_{asym}(CO₂) is essentially invariant between solid and solution phases indicating constancy of structure, while δ(¹¹⁹Sn) (–84.9 to –121.9 p.p.m.) is more typical of (I) [e.g. O(SnPh₃)₂, –83.6 p.p.m.¹⁰] than (II) [e.g. SnPh₃(dppd), –221.2 p.p.m.; dppd = 1,3-diphenylpropane-1,3-dionate¹⁰].

These data suggest that these compounds are tetrahedral at tin in both phases, and that chelation by the carboxylate group to form a *cis*-SnR₃O₂ structure is absent or, at best, weak.^{6,7,11} On the other hand, (18)–(22) have enhanced q.s. values (3.49–3.71 mm s⁻¹), typical of the *trans*-SnR₃O₂ structure (III).¹³ This polymeric structure is disrupted upon dissolution to yield

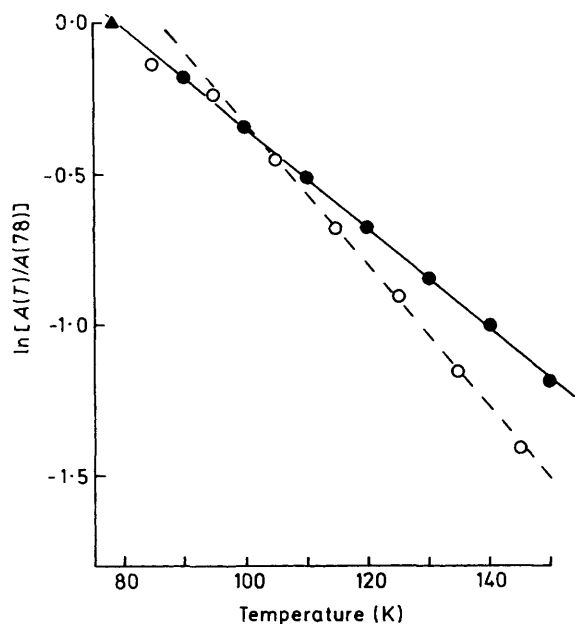


Figure 1. Variable-temperature Mössbauer spectroscopic data for (12) (●) and (21) (○). In the latter case, the best-fit linear regression is for $T \geq 95$ K (see text). The point ▲ is common to both plots

tetrahedral monomers (I) [δ (^{119}Sn) -102.1 to -106.3 p.p.m.], a change which is also reflected in a shift of *ca.* 100 cm^{-1} to higher frequency in the position of $\nu_{\text{asym}}(\text{CO}_2)$ on going from solid to solution phases.

In addition, we have examined the variable-temperature Mössbauer spectroscopic (v.t.M.s) behaviour of two isomers (12) ($X_n = 2,5\text{-Cl}_2$) and (21) ($2,4\text{-Cl}_2$) which are representative of these two compound groupings. We have shown previously¹⁴ that in plots of $\ln[A(T)/A(78)]$ vs. T ($A =$ Mössbauer spectral area at temperature T , normalised to 78 K to facilitate intersample comparison), essentially linear data sets are recorded whose slope ($a = -d \ln A/dT$) is a measure of the lattice rigidity, as perceived by the Mössbauer-active nucleus. Lower values of a indicate a more rigid lattice, which is in turn dependent upon (i) monomer vs. polymer formation, (ii) the strength of the intermolecular bonds within the polymer chain, and (iii) the spacial disposition of SnR_n and the bridging ligands. Data for the two compounds studied are given in Figure 1.

For (12), which is essentially tetrahedral at tin (see above) and hence must form a non-associated lattice, the $\ln[A(T)/A(78)]$ vs. T plot is linear over the entire T range studied (78–150 K) and has $10^2a = 1.67\text{ K}^{-1}$ (regression coefficient = -0.999 , 8 points). This a value is entirely consistent with a molecular lattice [e.g. $\text{O}(\text{SnPh}_3)_2$, $10^2a = 1.56$;¹⁴ $\text{SnPh}_3(\text{O}_2\text{CC}_6\text{H}_4\text{N}_2\text{R}''\text{-}o)$ ($\text{R}'' = 2\text{-hydroxynaphthyl}$), $10^2a = 1.60\text{ K}^{-1}$].⁸ Data for (21) show some curvature, particularly at $T < 95$ K, which we ascribe to vibrational anharmonicity within the lattice rather than thickness effects, since for both (12) and (21) samples containing *ca.* $1.0\text{ mg }^{119}\text{Sn cm}^{-2}$ were used in the study. Slope data in the 95–145 K range are $10^2a = 2.34\text{ K}^{-1}$ (-0.999 , 6 points), or over the whole T range studied 2.10 K^{-1} (-0.946 , 8 points), but regardless of how the data are analysed the conclusions are the same. For such a strong temperature dependence of the spectral area to be consistent with a molecular lattice, as for (12), then to maintain a *trans*- SnR_3O_2 geometry at tin (from q.s. data) the compound must form small cyclic oligomers, as, for example, $\{\text{SnPh}_3[\text{O}_2\text{P}(\text{OPh})_2]\}_6$.¹⁵ However, such a structure should manifest itself in solution, for

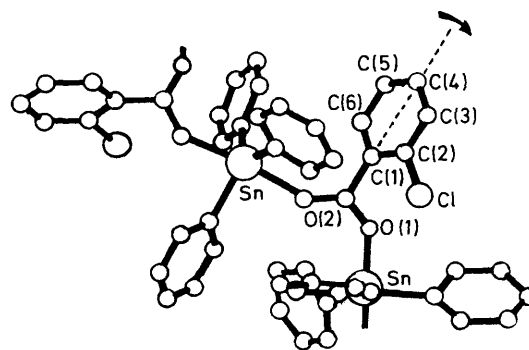


Figure 2. Schematic representation of the general structure of triphenyltin benzoates, including the atomic numbering scheme used in the text

example in ^{119}Sn n.m.r. chemical shifts or linewidths, which should show some indication of $c.n. = 4/c.n. = 5$ equilibria ($c.n. =$ co-ordination number). That no such observations are made rules out this hypothesis. The v.t.M.s. data are also consistent with a chain structure, provided that the three-dimensional arrangement of tin and bridging ligands is coiled, *i.e.* S-shaped (Class 3) or helical (Class 4).¹⁴ This interpretation is readily reconciled with the local stereochemistry at tin, and data can be compared with $\text{SnPh}_3(\text{O}_2\text{CMe})$, which is also a Class 3 polymer, where $10^2a = 1.91\text{ K}^{-1}$. From our experience with studies of triphenyltin acetate and formate, and assessments of the structures of organotin derivatives of aliphatic carboxylic acids,⁴ 'coiling' in Class 3 polymers of this type arises to minimise steric interactions between the R' group of the acid (in the current context $\text{C}_6\text{H}_5\text{-}X_n$) and the hydrocarbons on tin (*i.e.* Ph). V.t.M.s. data for (21) suggest that these steric interactions are quite significant (hence marked coiling within the polymer chain and high a value) and could, in severe cases, lead to molecular rather than polymeric structures.

In order to rationalise the factors which influence the choice of structure within this series of compounds, we have included in Table 2 calculated $\text{p}K_a$ values (25°C , H_2O) of each benzoic acid as an indicator of the electronic properties of the ligand.* This parameter will reflect the inductive and mesomeric effects of the aromatic ring substituents, and will, in essence, provide a measure of the electronegativity of the $-\text{CO}_2\text{R}'$ group. Clearly, while the $\text{p}K_a$ of the acid in H_2O will not totally reflect its behaviour in other media, particularly organic solvents, other available equations for calculating $\text{p}K_a$ would only change the absolute value of this parameter and not the relative ordering of acid strengths (electronegativity).

From Table 2, it can be seen that the molecular structures (1)–(17) are formed by compounds containing the weakest, or least electronegative, of the acids, with $\text{p}K_a > 3.0$. There are two exceptions to this observation [(12), $X_n = 2,5\text{-Cl}_2$, $\text{p}K_a = 2.55$; (17), $3,5\text{-(NO}_2)_2$, 2.72], and in both cases the aromatic ring of the acid bears substituents on either side of the C(1)–C(4) axis. This situation is shown diagrammatically in Figure 2, using the positional parameters for $\text{SnPh}_3(\text{O}_2\text{CC}_6\text{H}_4\text{Cl-}2)$ taken from ref. 11. The crystallographic data show that the substituted ring is rotated about C(1)–C(4) to move the chlorine away from the phenyl groups of the intermolecularly bonded tin, thereby minimising the major steric interaction. However, the hydrogen atoms on C(6), and to a lesser extent C(5), also sterically interact with the phenyl groups on the adjacent tin, which is accommodated in part by opening of the angles at O(1) and O(2), but more significantly by a rotation about C(1)–C(4). This

* Calculated using $\text{p}K_a = 4.20 - \Sigma\sigma$. Hammett σ values are taken from ref. 16.

is an unfavourable event, since conjugation between CO₂ and the aromatic ring is diminished, and in the case of the 2-chlorobenzoate (**18**) leads to a dihedral angle between the two parts of the acid ligand of 60.6°. While the original authors¹¹ ascribe this angle to the steric requirements of C(1) and O(1) within the ligand, the dihedral angle in the free acid between O(2) (*i.e.* hydrogen bonding is not influencing structure) and Cl is only 13.7°,¹⁷ which we take as evidence that the non-planarity within the acid is arising largely from intermolecular factors, as described above.

In the context of the 'anomalous' structures for (**12**) and (**17**), the steric problems previously discussed are maximised by having substituents on either side of the C(1)–C(4) vector, and thus in these two compounds the monomeric structures are dictated by steric factors. However, for the remaining acids in this group, with the exception of (**14**) ($X_n = 3,5\text{-Cl}_2$), it is hard to visualise any greater steric demands for the ring substituents than in the case of (**18**) ($X_n = 2\text{-Cl}$), and so the molecular structures adopted by (**1**)–(**11**), (**13**), (**15**), and (**16**) must be determined by electronic factors, while in the case of (**14**) both steric and electronic factors act in unison. The contrast between monomeric (**7**) ($X_n = 2\text{-F}$, $pK_a = 3.27$) and polymeric (**18**)–(**20**) ($X_n = 2\text{-Cl}$, 2-Br , 2-I ; $pK_a = 2.92, 2.85, 2.86$ respectively) is most vivid.

Compounds (**18**)–(**22**) all incorporate strongly electronegative acid ligands ($pK_a < 3.0$), and being free from steric crowding on either side of the C(1)–C(4) axis, all adopt polymeric structures, dictated now by electronic factors and rationalised in a similar argument to that presented above for the series of 2-halogenobenzoic acid ligands.

In what way then does the electronegativity of the ligand influence the structure of triorganotin compounds? Most obviously, the more electron withdrawing the ligand the greater the Lewis acidity at tin and thus the likelihood of *c.n.* = 5 (whatever the geometry at tin) is maximised. Such an argument alone is, however, too simplistic. Why, for example, do compounds (**12**) and (**17**) not form *clearly* chelated structures (**II**)? Moreover, why is it that the structural chemistry of SnMe₃(L–L) (L–L = bidentate ligand) has only one crystallographically authenticated example of a *cis*-SnR₃L₂ geometry and one with *c.n.* = 4 against over 20 *trans*-SnR₃L₂ examples, while for SnPh₃(L–L) five compounds have the *trans*-SnR₃L₂ arrangement compared with 14 which have either *cis*-SnR₃L₂ or *c.n.* = 4 stereochemistries,^{6–8,11,12,18} this despite the fact that on simple inductive effect grounds –SnPh₃ should be more Lewis acidic than –SnMe₃?

In agreement with Holmes *et al.*,⁷ we believe that the relative electronegativities of Me, Ph, and L–L need to be considered, in the light of the positions within the trigonal-bipyramidal framework each of these groups is required to occupy in the two five-co-ordinated isomers. In simple hybridisation terms,¹⁹ the most electronegative ligands occupy the axial positions, while the more electropositive groups lie in the equatorial sites, bonded to tin by *s*-dominated orbitals. Structure (**II**) is thus disfavoured for R = Me, since Me is rarely likely to be more electronegative than L, which usually involves donors such as O, N, and S. Moreover, the large electronegativity difference between Me and typical O, N, S-donor ligands is likely to be best accommodated by the polarised bonding scheme of the *trans*-SnR₃L₂ geometry (**III**). Conversely, (**II**) is likely to be favoured in the case of R = Ph by its enhanced electronegativity,²⁰ which is more in keeping with the electronegative L groups. In order for the polymeric structure (**III**) to be adopted when R = Ph, the electronegativity of the ligand L–L must be significantly greater than that for Ph in order to encourage the latter to involve an orbital of otherwise unfavourable *s* content in its bonding. It is this factor which is evident in the structures of (**18**)–(**22**).

The reason for the largely tetrahedral nature of (**1**)–(**17**), and

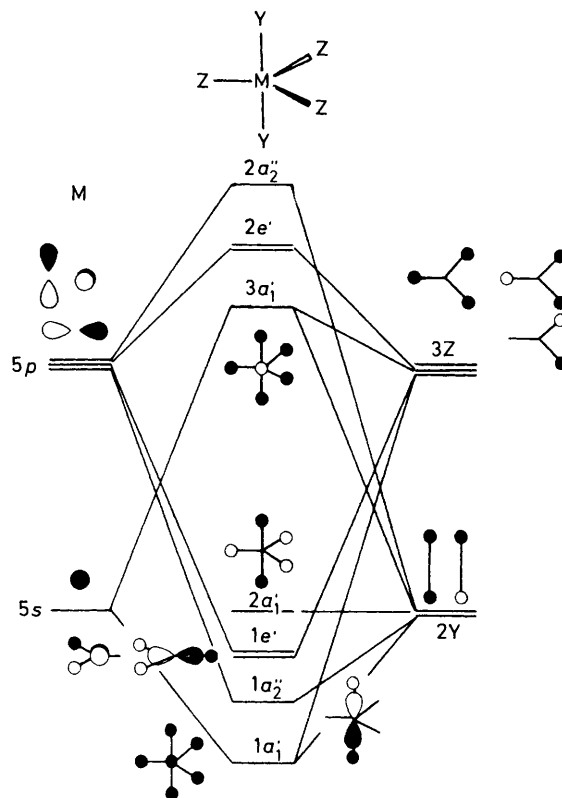


Figure 3. Molecular orbital energy level diagram for *trans*-MZ₃Y₂ (*D*_{3h})

of (**12**) and (**17**) in particular, can only be speculated. Since the O₂CR' ligands in the last two would presumably prefer structure (**III**) in the absence of steric effects, it is plausible that it is one of the highly electronegative oxygen atoms that is reluctant to involve an *s*-dominated equatorially oriented orbital on tin, and that the only available alternative is the tetrahedral geometry which allows a more equitable mix of *s* and *p* character in the four bonding orbitals on tin, a situation which in turn is suited to those acids of high pK_a , where the electronegativities of Ph and O are more similar. It should also be noted that chelation involving four-membered rings involves greater strain than cases in which a five-atom ring is formed, and it is noteworthy that the best examples of the *cis*-SnR₃L₂ configuration for R = Ph, and indeed the only example for R = Me,²¹ occur in these latter circumstances.

Similar conclusions regarding the influence of the electronegativities of R and L can be arrived at by molecular orbital (m.o.) considerations. The qualitative m.o. diagram for an idealised *trans*-MZ₃Y₂ (*D*_{3h}) system is shown in Figure 3 and is arrived at by a combination of planar MZ₃ with linear Y₂. A similar analysis applied to PH₅ has been made by Hoffmann *et al.*²² No attempt is made in this analysis to quantify the overlap integrals, nor are the π -bonding effects included. The aim of this and subsequent diagrams is to indicate the *relative* m.o. energies for different geometrical arrangements and how they may be controlled by Z and Y electronegativities. The absolute value of the orbital energies and indeed their relative ordering are thus of secondary importance in what we consider to be a 'first approximation' analysis. For comparison, typical values of the atomic orbital (a.o.) energies are for Sn(5s, 5p) –16, –8; C(*sp*² or *sp*³) –13; O(*sp*²) –20; S(*sp*²) –14 eV.²³ The relative ordering of Z and Y energies in Figures 3–6 is made on the basis that equatorial ligands Z are generally less electronega-

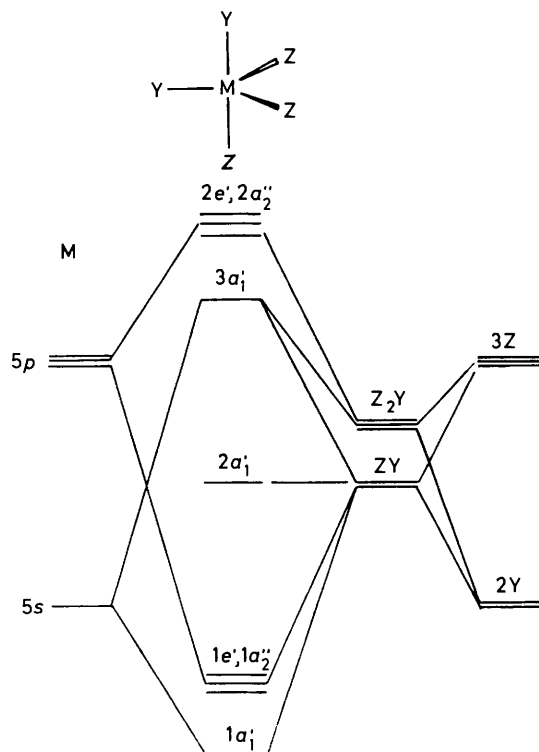


Figure 4. Molecular orbital energy level diagram for *cis*- MZ_3Y_2 (C_s). The labelling of Figure 3 is retained for comparative purposes only. The relative ordering within the $1e'$, $1a_2''$ m.o.s and the corresponding group of antibonding orbitals is uncertain

tive than axial ligands Y. While this could be construed as 'anticipating the answer', it in no way affects the overall interpretation of this set of diagrams.

In the D_{3h} system (Figure 3) the ten available electrons fill the $1a_1'$, $1a_2''$ and degenerate $1e'$ bonding m.o.s along with the non-bonding $2a_1'$ m.o. in which electron density resides solely on the ligands. Although equal contributions from all five ligand a.o.s are implied in the pictorial representation of this m.o. shown in the figure, calculations for PH_5 show that the a.o.s of the two axial Y ligands dominate. While the electronegativities of both Z and Y, and hence the valence orbital ionisation energies of these atoms, will influence the energies of these five m.o.s it seems reasonable that the non-bonding $2a_1'$ orbital, dependent as it is solely on the electronegativity of Y, will be most influenced. The more electronegative is Y, the lower the $2a_1'$ energy and hence the more stable the D_{3h} geometry. This is the m.o. equivalent to the 'axially most electronegative' analysis of Bent.¹⁹

For the *cis*- MZ_3Y_2 (C_s) system the symmetry is lowered, but the appearance of the m.o.s is essentially unchanged because the symmetry of the valence σ orbitals is the same as for D_{3h} (Figure 4). (The labelling of the m.o.s has been retained from the D_{3h} diagram for comparative purposes, but these labels no longer strictly apply.*) The most obvious effect of producing symmetry-adapted axial ZY orbitals, whose energy is intermediate between Z and Y, is that the non-bonding $2a_1'$ orbital is higher in energy than for the D_{3h} case. While this implies that the C_s symmetry will always be less favourable than D_{3h} , the former becomes most viable when the energies (electronegativities) of Z and Y are close, *i.e.* mixing Z, Y energy

* For example, the pair of predominantly equatorially bonded m.o.s designated e' are no longer degenerate under C_s symmetry.

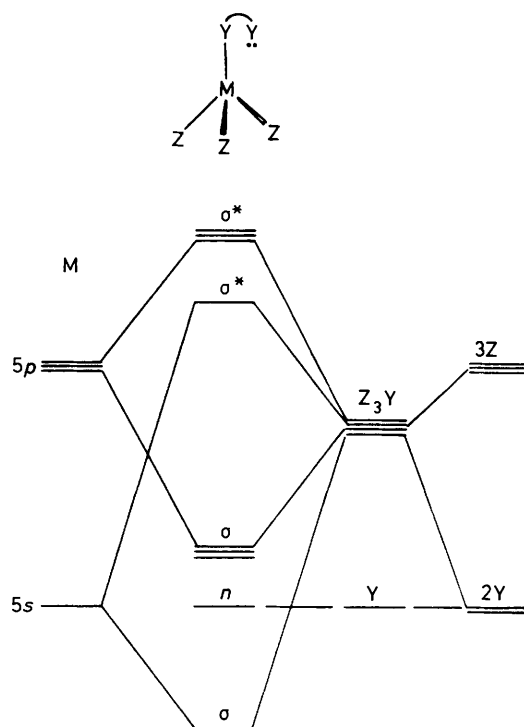


Figure 5. Molecular orbital energy-level diagram for a tetrahedral triorganotin bonded to a bidentate Y-Y ligand

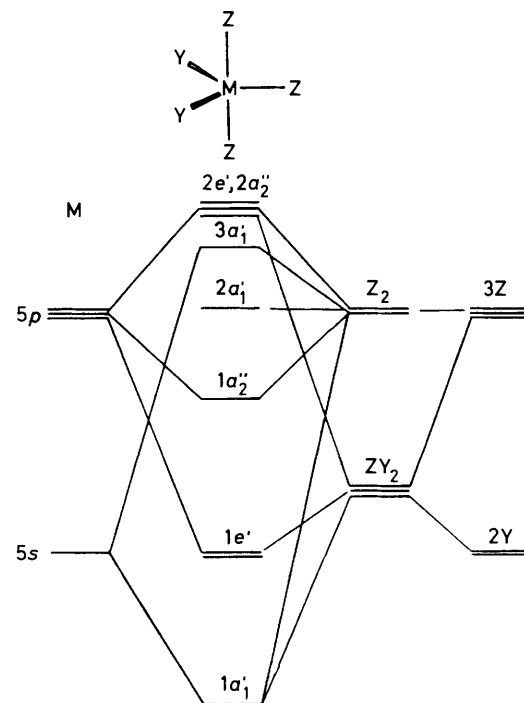


Figure 6. Molecular orbital energy-level diagram for *mer*- MZ_3Y_2 (C_{2v}). The orbital labelling is for comparison with Figure 3 only. The ordering of energy levels is uncertain

levels minimises the extent to which $2a_1'$ is raised in energy. Thus X = Ph rather than Me, and Y = S or low-electronegativity O ligands favour the *cis* structure.

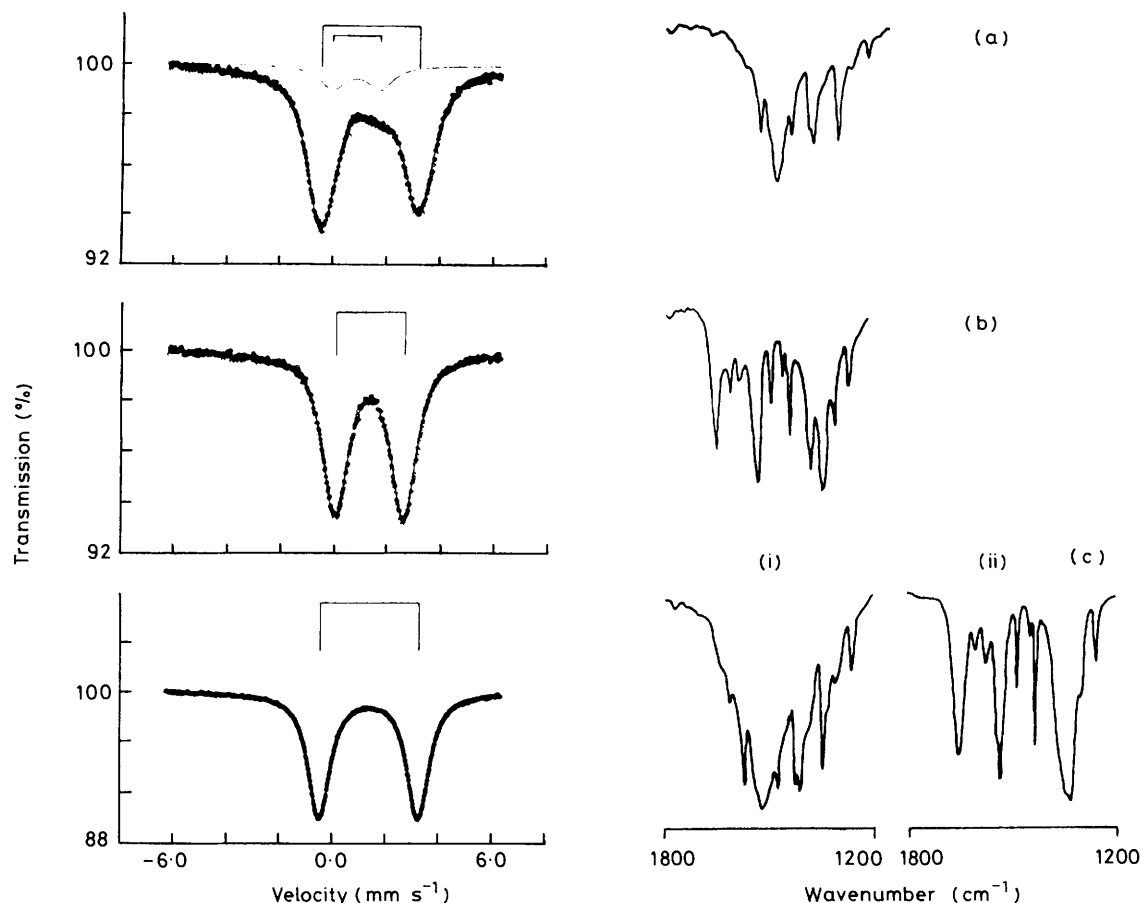


Figure 7. Mössbauer and i.r. spectra (KBr disc or CCl_4 solution) of (a) crude (24). The minor component of the Mössbauer spectrum (i.s. = 0.77, q.s. = 1.79 mm s^{-1}) is most probably SnPh_2O . (b) (24a) and (c) (24b), including (i) solid and (ii) solution state i.r.

For those cases where Y is a strongly electronegative ligand but steric factors preclude D_{3h} (*trans*- MZ_3Y_2) symmetry, the *cis* arrangement is particularly unfavourable. However, by forming a four-co-ordinate tetrahedral complex one of the axial Y orbitals becomes non-bonding, and because it is no longer required to mix with the orbital of axial Z, it is not raised in energy (Figure 5).^{*} Thus, despite conditions of favourable Lewis acidity at M, sterically precluded *trans*- MZ_3Y_2 isomers are likely [as with (12) and (17) herein] to revert to tetrahedral rather than *cis*- MZ_3Y_2 structures.

The final pair of compounds, (23) and (24), generate less clear-cut structural data than the previous two groupings, but the overall picture which emerges is entirely in keeping with the discussions presented above. The two ligands from which (23) and (24) are formed are the most acidic (electronegative) of the series studied, with $\text{p}K_a < 2.4$. However, these two ligands are also among the most sterically demanding, with bulky, electron-withdrawing ring substituents in the 2-[(24)] or 2,6-positions [(23)]. Under these circumstances, electronic factors strongly favour the polymeric structure (III), while steric factors clearly will resist the formation of such an arrangement.

For the 2- NO_2 compound (24), preparation in either toluene or acetone yields a crude product (after solvent evaporation) whose Mössbauer spectrum consists mainly of a doublet (isomer shift, i.s. = 1.30 , q.s. = 3.68 mm s^{-1}) and whose i.r. spectrum is dominated by an intense broad band at 1520 cm^{-1}

(Figure 7). When this material is purified by recrystallisation from light petroleum (b.p. $40\text{--}60^\circ\text{C}$) to which enough acetone was added to bring about dissolution, the polymeric product (24b) crystallises,[†] with traces of included solvent. The Mössbauer q.s. (3.70 mm s^{-1}) and solid- and solution-state i.r. data ($1520, 1653 \text{ cm}^{-1}$) are unambiguously assigned to structural type (III). However, when the crude product is recrystallised from toluene-petroleum (b.p. $40\text{--}60^\circ\text{C}$), spectroscopic data suggest a monomeric structure (I) [(24a): q.s. = 2.58 mm s^{-1} ; i.r. (solid, solution): $1645, 1650 \text{ cm}^{-1}$]. The two sets of data are linked by the ^{119}Sn n.m.r. data. For (24a) this is -92.8 p.p.m., while (24b), although much less soluble (in keeping with its proposed structure), has a virtually identical chemical shift of -91.6 p.p.m. The difference in these two values may arise from either concentration effects and/or solvent effects from traces of solvent included in the solid lattice.

These data suggest that a delicate balance between structural and electronic factors exists in this case, with included-solvent stabilisation of the lattice being a possible arbitrating factor.

One previous claim for monomer/polymer isomers of an organotin compound exists in the literature.²⁴ A freshly prepared sample of $\text{SnPh}_3(\text{O}_2\text{CCl}_3)$ was found to have Mössbauer and i.r. data consistent with a tetrahedral geometry at tin, while a 5 year old sample showed both monomer and polymer isomers. An independent synthesis of the polymer form has also been reported.²⁴ While we have not observed any solid-

^{*} For a pictorial representation of the four symmetry-adapted ligand orbital combinations see, for example, ref. 23, p. 154.

[†] Mention of preliminary X-ray data for a polymeric form of $\text{SnPh}_3(\text{O}_2\text{CC}_6\text{H}_4\text{NO}_2)_2$ has recently been made.¹¹

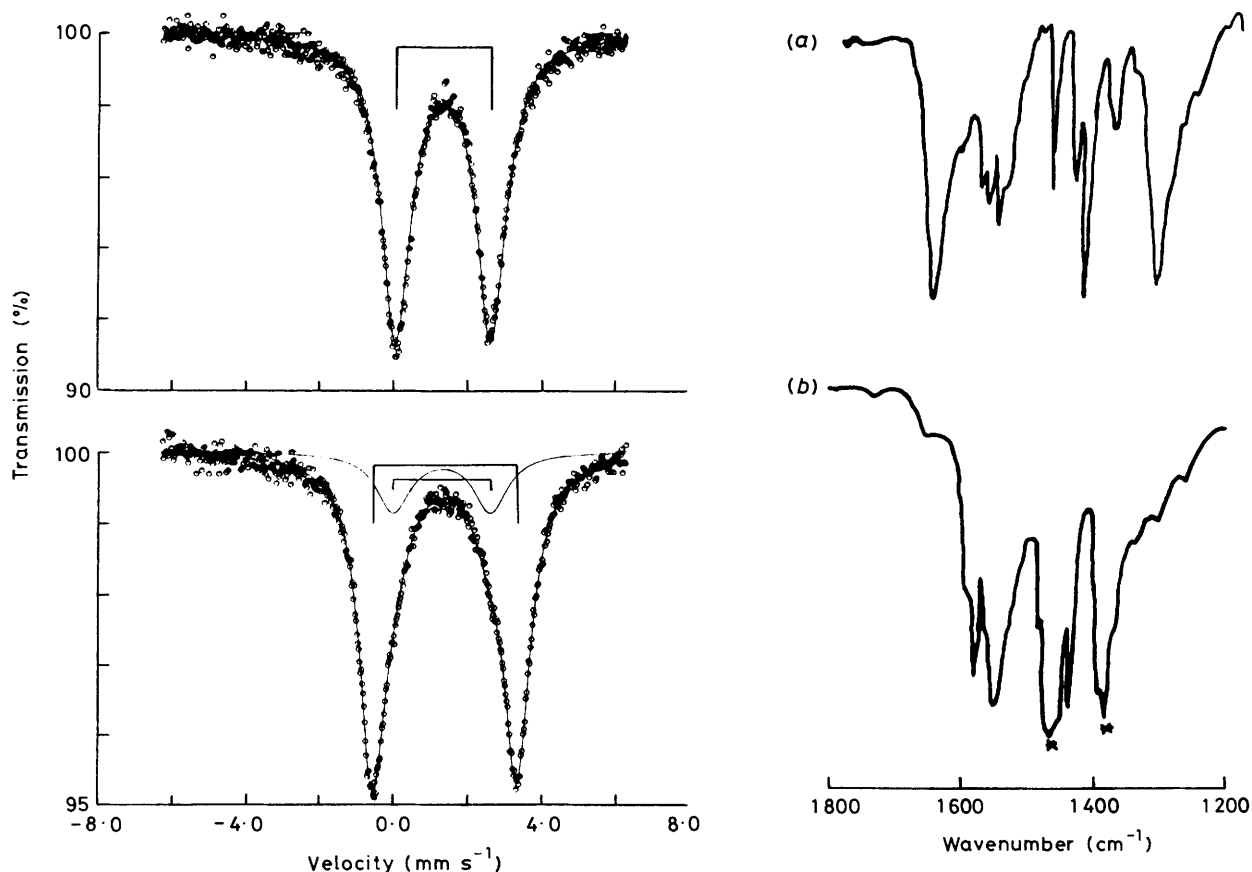


Figure 8. (a) Mössbauer and i.r. spectra (KBr disc) of (23). (b) Related spectra of a Nujol mull of (23). Bands marked * arise from the mulling agent

state isomerisation between (24a) and (24b), it is noteworthy that the ligand characteristics of the trichloroacetate are the same as the 2-nitrobenzoate: strong electron-withdrawing group(s) (high electronegativity) combined with substantial steric demand.

The spectroscopic data for the 2,6-dichlorobenzoate (23) follow a similar, though less conclusive, pattern to those of (24). Recrystallisation of the crude product from acetone-cyclohexane yields a product whose spectroscopic data (Figure 8) are clearly indicative of the monomeric structure (I) [i.r. (KBr disc, solid; solution), $\nu_{\text{asym}}(\text{CO}_2)$: 1 653, 1 660 cm^{-1} ; q.s. = 2.57 mm s^{-1} ; $\delta(^{119}\text{Sn})$ -93.0 p.p.m.]. However, quite remarkably, when the i.r. spectrum of this recrystallised material is recorded as a Nujol mull, $\nu_{\text{asym}}(\text{CO}_2)$ shifts by 100 cm^{-1} to 1 545 cm^{-1} . Moreover, a Mössbauer spectrum of the Nujol mull is dominated by a doublet with i.s. = 1.39, q.s. = 3.89 mm s^{-1} , and only a small contribution from the monomer structure with parameters i.s. = 1.29, q.s. = 2.62 mm s^{-1} . While such evidence cannot be taken as definitive, the implications are clearly that in a Nujol matrix, the 2,6-dichlorobenzoate ligand is bidentate, with the overall triphenyltin complex having structure (III) in a polymeric or possibly oligomeric formulation. These results endorse the delicate balance between monomeric and oligomeric structures under circumstances where the competition between steric and electronic influences is most acute.

Finally, in the light of this discussion it is worth considering the electronic factors which will enable formation of the *mer*- MZ_3Y_2 geometry, which is yet to be crystallographically authenticated in organotin chemistry.

Figure 6 shows the qualitative m.o. diagram for the *mer*-

MZ_3Y_2 isomer. Again, despite lower symmetry here (C_{2v}) than for *trans*- MZ_3Y_2 , the symmetry of the ligand σ -orbitals is essentially preserved and the picture is similar to that for the D_{3h} case. The (incorrect) orbital labels have been retained from Figure 3 for comparison. The major difference between Figures 3 and 6 is the energy of the non-bonding $2a_1'$ and to a lesser extent the bonding $1a_2''$ m.o.s, both of which will be raised in energy since they originate from the less electronegative Z atomic orbitals. The orbital energetics thus confirm the experimental fact that this will be an unusual isomer as far as organotin chemistry is concerned. We predict that the best chance for securing this geometric arrangement is with a highly electronegative Z (to lower $2a_1'$ and $1a_2''$) and a weakly electronegative Y (so it does not compete too strongly with Z for the axial sites). For example, $\text{Sn}(\text{C}_6\text{F}_5)_3(\text{S}_2\text{CNMe}_2)$ might be a possibility.

In conclusion, can we reiterate that these m.o. diagrams serve only to suggest the origins of structural preference. No account is taken of detailed orbital energies, extents of overlap, π -bonding effects, bond energies, weak intermolecular interactions and lattice energies in general, ring strain in chelated systems or kinetics (which will favour chelates over bridging ligands), all of which will be of importance. We hope by this contribution simply to stimulate interest in how electronic factors can be utilised to influence the structure of organotin compounds.

Acknowledgements

We (S. J. B. and R. H.) thank the International Tin Research Institute, London, for permission to publish these results.

References

- 1 Part 10, K. C. Molloy, T. G. Purcell, D. Cunningham, P. McCardle, and T. Higgins, *Appl. Organomet. Chem.*, 1987, **1**, 119.
- 2 R. C. Poller, *J. Organomet. Chem.*, 1965, **3**, 321.
- 3 B. F. E. Ford, B. V. Liengme, and J. R. Sams, *J. Organomet. Chem.*, 1969, **19**, 53.
- 4 K. C. Molloy, K. Quill, and I. W. Nowell, *J. Chem. Soc., Dalton Trans.*, 1987, 101.
- 5 K. C. Molloy, T. G. Purcell, F. E. Hahn, H. Schumann, and J. J. Zuckerman, *Organometallics*, 1986, **5**, 85.
- 6 R. G. Swisher, J. F. Vollano, V. Chandrasekhar, R. O. Day, and R. R. Holmes, *Inorg. Chem.*, 1984, **23**, 3147.
- 7 J. F. Vollano, R. O. Day, D. N. Rau, V. Chandrasekhar, and R. R. Holmes, *Inorg. Chem.*, 1984, **23**, 3153.
- 8 P. G. Harrison, K. Lambert, T. J. King, and B. Majee, *J. Chem. Soc., Dalton Trans.*, 1983, 363.
- 9 S. J. Blunden, P. J. Smith, and B. Sugavanam, *Pestic. Sci.*, 1984, **15**, 253.
- 10 K. C. Molloy, K. Quill, S. J. Blunden, and R. Hill, *Polyhedron*, 1986, **5**, 959.
- 11 R. R. Holmes, R. O. Day, V. Chandrasekhar, J. F. Vollano, and J. M. Holmes, *Inorg. Chem.*, 1986, **25**, 2490.
- 12 K. C. Molloy, T. G. Purcell, K. Quill, and I. W. Nowell, *J. Organomet. Chem.*, 1984, **267**, 237.
- 13 A. G. Davies and P. J. Smith, in 'Comprehensive Organometallic Chemistry,' ed. G. Wilkinson, Pergamon, New York, 1982, p. 525.
- 14 K. C. Molloy and K. Quill, *J. Chem. Soc., Dalton Trans.*, 1985, 1417.
- 15 K. C. Molloy, F. A. K. Nasser, C. L. Barnes, D van der Helm, and J. J. Zuckerman, *Inorg. Chem.*, 1982, **21**, 960.
- 16 D. D. Perrin, B. Dempsey, and E. P. Serjeant, 'pK_a Predictions for Organic Acids and Bases,' Chapman and Hall, London and New York, 1981.
- 17 G. Ferguson and G. A. Sim, *Acta Crystallogr.*, 1961, **14**, 1262.
- 18 P. A. Cusack, P. J. Smith, J. D. Donaldson, and S. M. Grimes, 'A Bibliography of X-Ray Crystal Structures of Tin Compounds,' Publication No. 533, International Tin Research Institute, Uxbridge, 1981.
- 19 H. A. Bent, *Chem. Rev.*, 1961, **61**, 275.
- 20 J. E. Huheey, 'Inorganic Chemistry,' 3rd edn., Harper and Row, New York, 1983, p. 156.
- 21 P. G. Harrison, T. J. King, and K. C. Molloy, *J. Organomet. Chem.*, 1980, **185**, 199.
- 22 R. Hoffmann, J. M. Howell, and E. L. Muetterties, *J. Am. Chem. Soc.*, 1972, **94**, 3047; T. A. Albright, J. K. Burdett, and M. H. Wangbo, 'Orbital Interactions in Chemistry,' Wiley-Interscience, New York, 1985.
- 23 W. W. Porterfield, 'Inorganic Chemistry, A Unified Approach,' Addison-Wesley, 1984, p. 53.
- 24 B. F. E. Ford and J. R. Sams, *Inorg. Chim. Acta*, 1978, **28**, L173.

Received 15th April 1987; Paper 7/691